ACS APPLIED MATERIALS & INTERFACES

Research Article

www.acsami.org

Facile and Universal Superhydrophobic Modification to Fabricate Waterborne, Multifunctional Nacre-Mimetic Films with Excellent Stability

Qiong Wu, Dan Guo, Youwei Zhang, Hewei Zhao, Dezhi Chen, Jianwei Nai, Junfei Liang, Xianwu Li, Na Sun, and Lin Guo*

School of Chemistry and Environment, Beihang University, Beijing 100191, China

Supporting Information

ABSTRACT: Although numerous kinds of waterborne, nacre-mimetic films with excellent properties have been fabricated via different assembly methods, it remains difficult to put those kinds of lightweight materials into practical applications because they are sensitive to water in the environment. Herein, a simple superhydrophobic modification method was used to enhance the repellency of film to water and/or corrosive liquids in the environment. Furthermore, it lowered the gas transmission rate of the films dramatically and improved the heat and flame shield capabilities. This approach could also be applied to other kinds of nacre-mimetic films, proving to be a versatile, low-cost, fast, and facile method to produce large-area and thick, waterborne, multifunctional films with excellent repellency to water and some corrosive liquids in the environment, which will pave the road for the practical applications of nacre-mimetic films.

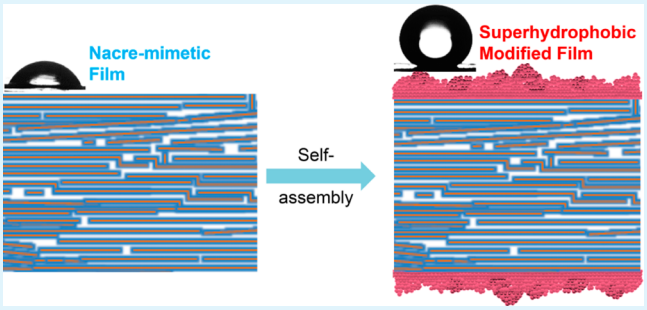

KEYWORDS: *nacre-mimetic, superhydrophobic, repellency, gas barrier, heat and flame shield*

INTRODUCTION

Quite often, nature could produce lightweight materials with robust stability and excellent properties in simple components at low cost,[1−4] for example, nacre, bone, spider silk, and tooth. Thus, scientists and engineers have long been taking lessons from nature to manufacture lightweight materials with superior properties, which undoubtedly are needed in a wide area of fields.[5−8] Among all the biological materials, nacre has gained tremendous interest because it has exceptional stability and excellent properties owing to its unique brick-and-mortar structure, constituted of highly aligned inorganic platelets surrounded by a protein matrix that serves as a glue between the platelets.[9−11] A great amount of bioinspired research has been extensively investigated to produce nacre-mimetic materials,[12−16] such as inorganic platelet-reinforced composites (Al_2O_3,[17−20] clay,[21−26] LDH (layered double hydroxide), etc.[27−30]) and carbon-reinforced composites (graphene,[31] graphene oxide (GO),[32−34] carbon nanotubes (CNTs),[35,36] etc.).

Probably the most studied are the clay/waterborne polymer composites, such as montmorillonite (MTM)/poly(vinyl alcohol) (PVA) and montmorillonite (MTM)/poly(diallyldimethylammonium) chloride (PDDA), because MTM is naturally abundant, is cheap, and possesses many exceptional properties, for example, distinguished thermal shield capabilities. Also, the waterborne polymer is compatible to the nanoclay and moreover very attractive for environmental reasons. Up to now, MTM nacre-mimetic composites with excellent properties have been successfully fabricated in different compositions[5,22,26] and component content[21,25,37] at different scales via various assembly methods.[21,25,38−40]

However, industrial applications such as coatings for buildings and spaceships, not to mention biomedical implants, typically require robust repellency to water and/or some corrosive liquids in the environment and simplified low-cost fabrication procedures, besides superior properties. However, the waterborne components are very susceptible to water, leading to hydration-induced decay of various properties of the composite.[21,41] Thus, deposited water and/or corrosive liquid (such as rain and unintended sprayed liquid), which are common in the environment, will be inevitably detrimental to the performance of the composite. Although this phenomenon was discovered a long time ago and the problem is vital to advance the composites into practical applications, it has been ignored until recently. There are several methods that try to preserve the properties of the film after exposure to water.[42,43] However, those solutions are not satisfactory because it will take a long time for post-treatment (at least 24 h) or it is not suitable when the film is exposed to deposited water. Thus, we explored a faster and more efficient method to solve the

Received: January 16, 2014
Accepted: November 6, 2014
Published: November 6, 2014

problem with knowledge in wettability, that is, if the wettability of the nacre-mimetic film could be tuned into superhydrophobic and low adhesive, it might be effective to prevent the influence of deposited water and/or corrosive liquids to the nacre-mimetic films.

Herein, we used a universal and facile superhydrophobic modification, which could impart to the film exceptional repellency to deposited liquids (such as water, corrosive liquids, etc.) and improve other properties, such as better gas barrier and heat and flame shield properties. Uncross-linked MTM/PVA nacre-mimetic film is chosen because there are abundant hydrogen bonds in the MTM/PVA system, which may be most susceptible to water in the environment. If we could minimize the effect of water and other kinds of corrosive liquids to the performance of uncross-linked MTM/PVA film, the method will also work for other nacre-mimetic films, such as MTM/PDDA, cross-linked MTM/PVA, and GO/PVA.

Unlike methods relating to the covalent cross-links and ionic supramolecular bonds, which are time-consuming (usually 1 week or more), not highly efficient, and only limited for several kinds of polymers for cross-linking and may make the film brittle,[44,45] this superhydrophobic modification provides a fast, facile, "green", low-cost and universal method, a minimum of upscaled apparatuses, only one procedure for modification, involving benign ethanol solvent, and readily available components. Additionally, the method could be further applied to prepare other multifunctional integrated MTM composite films and GO composite films with great repellency to water and corrosive liquids in the environment. Hence, this low-cost, fast, and easy method can open up a universal and facile avenue to produce multifunctional integrated lightweight materials with excellent repellency toward deposited liquids in the environment.

EXPERIMENTAL SECTION

Fabrication of Nacre-Mimetic Paper. Nacre-mimetic paper was prepared according to the literature method.[25] In a typical procedure, a 0.5 wt % dispersion of MTM (Zhejiang Fenghong Clay Co., Ltd.) in Milli-Q water was stirred intensely for 1 week. Then, the solution was centrifuged to get MTM nanosheets. To absorb a monolayer of PVA (molecular weight (Mw) ≈ 85−124 kDa, Aldrich) on MTM nanosheets, the dispersion was slowly dripped into a magnetically stirred PVA solution. The mixed solution was stirred overnight to complete absorption of polymer, followed by centrifugation to remove excess polymer. The deposit was redispersed into Milli-Q water to form a colloidal solution. Afterward, nacre-mimetic paper was fabricated by vacuum filtration of the solution through a membrane filter with a pore size of 0.22 μm. The paper was further dried by air and removed from the filter. Then, the prepared paper was dried at 60 °C for 24 h while applying a slight force to avoid folding of the paper during the drying process.

Fabrication of Superhydrophobic Nacre-Mimetic Paper. First, 1 g of polystyrene granules (Mw = 192 000 g/mol, Aldrich) were dispersed by 30 mL of ethanol in a closed bottle. The 0.8 g of hydrophobic fumed silica nanoparticles (Aerosil R202, average particle size 14 nm, Evonik Degussa Co.) were further mixed and stirred for 30 min. Then, superhydrophobic nacre-mimetic paper was produced by dip-coating at a speed of ca. 0.5 cm s^{-1}. The coated one was dried at room temperature and then heated at 80 °C for 1 h, yielding a firm coating on the surface.

Characterization. Scanning electron microscopy (SEM, FEI Quanta 250 FEG) was performed, typically operating at an acceleration voltage of 5−10 kV. A thin Au layer was sputtered onto the samples prior to imaging. Contact angles were measured by OCA20 instrument contact angle system at room temperature. All the data was obtained by measuring more than five samples. Mechanical tests were carried out on a universal testing machine (AGS-X, Shimaszu Co. Ltd., Japan) equipped at a rate of 0.6 mm/min with a 5 N load cell. The sample were obtained as 3−4 mm wide and 12−20 mm long rectangular strips of the materials. The exact cross-sectional thicknesses were determined by scanning electron microscopy. All samples were measured at room temperature and an average humidity of 23%.

Thermal Conductivity Measurements. Thermal conductivities of the samples before they were exposed to flame were obtained by Hot Disk Thermal Constant Analysers-2500 at room temperature and 1 atm pressure. Three replicate were used in the thermal conductivity measurements for every sample.

Permeation Measurements. Gas permeation measurements were carried out with a home-built stainless steel permeation apparatus at relative humidity (RH) 55%.[46] A nacre-mimetic film to be measured was placed in the permeation cell between two rubber O-rings with a support screen. The free-standing film was put on a nanoporous Anodisc membrane filter in order not to be damaged by the gas flow. The surface area of the sample available for gas transporting was 2.8 cm^2. The thickness of the film without coating is 33 μm, whereas the one after coating is 40 μm. The membrane was placed in the cell at the high-pressure side of the pressure gradient. The pressure gradient that was applied to each membrane was 3.0 psi. After passing through the film, the gaseous permeant was directed into a glass U-tube flow meter (A_{col} = 1.0 cm^2). The volumetric flow rate of the gas was then measured by recording the time ($t = t_f - t_i$) that was required for a soap bubble to travel a set distance ($X_{col} = d_f - d_i$), thereby sweeping out a defined volume. Measurements were taken until steady-state values were achieved (typically 1−2 h). At least six volumetric flow rates were recorded for each film, and the mean and standard deviations were determined. The permeation rate, P (10^6 cm^3 cm^{-2} s^{-1} $cmHg^{-1}$), was calculated using

$$P = \frac{X_{col}A_{col}}{t\frac{76p}{14.7}A_{mem}} \times 10^6 \quad (1)$$

RESULTS AND DISCUSSION

A nacre-mimetic film with excellent repellency toward water in the environment was fabricated by two steps of self-assembly. First, core−shell nanoplatelets of MTM coated by PVA were self-ordered into layered nacre-mimetic structure. Then, fumed silica nanoparticles about 14 nm in diameter were self-assembled into hierarchical structures on the surfaces of the nacre-mimetic film to form a superhydrophobic and low adhesive layer on the surfaces of the film. Scheme 1 illustrated the facile strategy (the detail of the method could be seen in the experiment part). The superhydrophobic treatment used here is independent of the thickness and the size of the film. More

Scheme 1. Strategy to Fabricate Nacre-Mimetic Film with Excellent Properties: MTM Platelets (Orange) Coated by a Layer of PVA (Purple) Are Self-Assembled into Nacre-Mimetic Film via Vacuum Filtration; Then, Fumed Silica Nanoparticles (Blue) Are Self-Assembled into Protective Layers, Which Are Superhydrophobic and Low Adhesive, To Minimize the Influence of Water and Other Liquids in the Environment

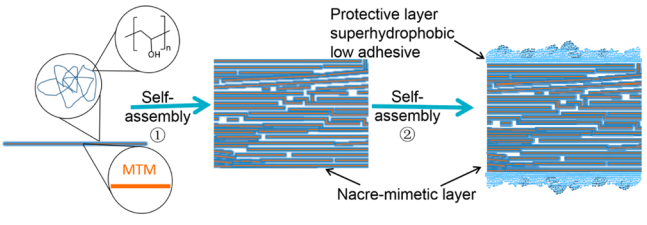

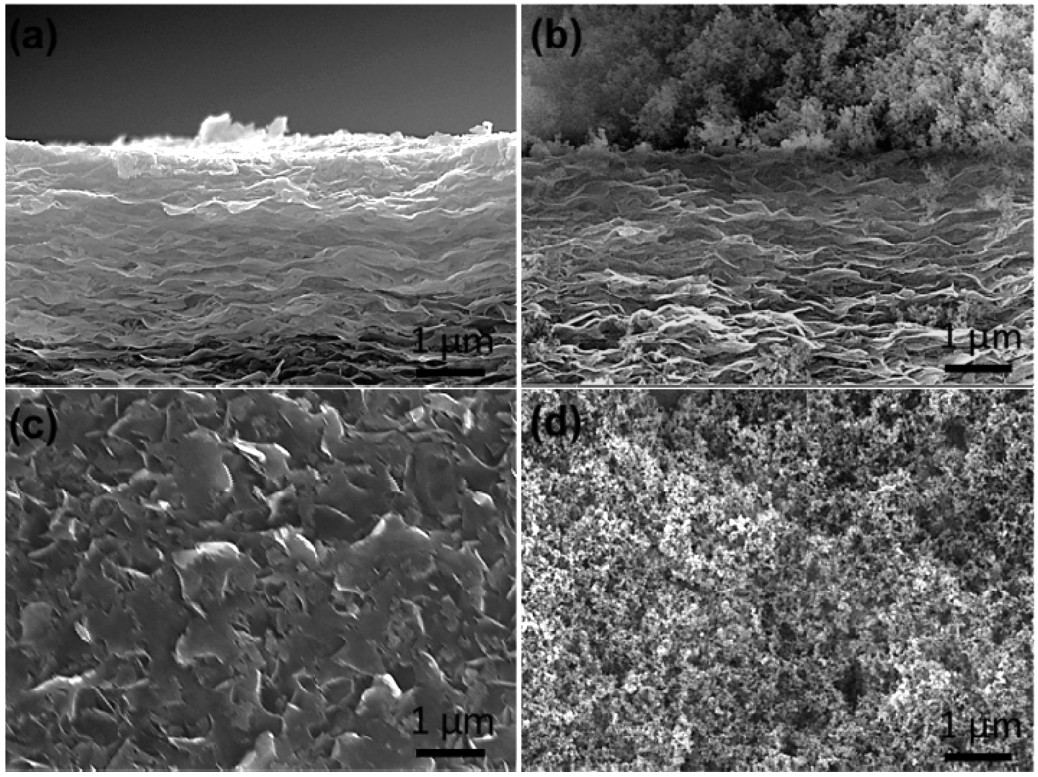

Figure 1. SEM images of the pure (a, c) and modified (b, d) MTM/PVA nacre-mimetic films, respectively. (a, b) Cross sections and (c, d) top-view images of the nacre-mimetic films.

importantly, the self-assembly time is very short. Thus, this method could be easily scaled up by simply adding more volume of as-prepared nanoparticle dispersion to the surfaces of larger films at almost the same time.

Scanning electron microscopy (SEM) was used to investigate the structure and surface morphology of the MTM/PVA nacre-mimetic film before and after modification (see Figure 1). Figure 1a revealed the film, consisting of 70 wt % MTM according to thermogravimetric analysis (TGA), with a well-defined layered structure, conceptually similar to the brick-and-mortar structure of nacre. Figure 1b showed part of the cross section of the modified film. By comparing parts a and b of Figure 1, it is obvious that the layered structure of the film was not affected by the modification. The only difference lies in that there is a layer (only about 3−4 μm in thickness) of silica nanoparticles with hierarchical structure on the surface of the nacre-mimetic film (see Figure 1b). The silica layer is so thin that the transparency of the film was almost preserved (see Figure 2a). The thickness of the film in Figure 2a without coating is 43 μm while the one with coating is 49 μm. In addition, Figure 1c, d showed the differences on the surface morphologies of the film before and after modification. The surfaces of pure nacre-mimetic film are rough, only on a micro scale, while there are obviously micro/nano-hierarchical structure on the surfaces of the modified one, consisting of fumed silica nanoparticles about 14 nm in diameter. As is known, the wettability of a film is primarily affected by its surface roughness and its surface energy. The self-assembly of silica aerogel particles formed a very thin layer with micro/nano structure. That lowered the surface energy by changing the component of the surfaces of the films as well as increased the surface roughness by forming a hierarchical structure on the surface.

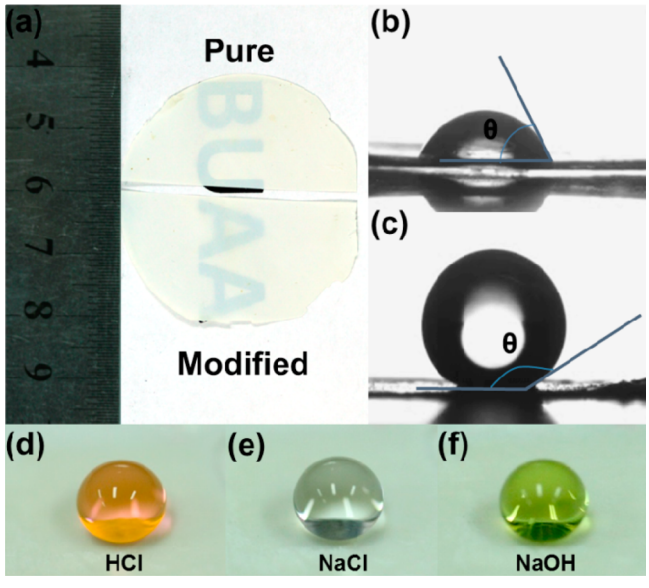

Figure 2. (a) Photographs of pure and modified MTM/PVA nacre-mimetic film. Optical images of droplets (b) on pure nacre-mimetic film and (c) on modified nacre-mimetic film. (d, e, f) Different kinds of corrosive liquid droplets with spherical shapes on the modified MTM/PVA films: (d) HCl droplet, (e) NaCl droplet, and (f) NaOH droplet.

To show a comprehensive effect of coating on the film clearly, we compared various properties of films before and after coating. Above all, the excellent stabilities of the modified films to water and corrosive liquids were investigated. In our experiment, water, HCL, NaOH, and NaCl droplets were used to mimic water, corrosive liquids, etc. in the environment. As

expected, after the modification, the MTM/PVA film exhibited superior repellency toward water and corrosive liquids. The contact angle of the modified film to water is 151.5° ± 0.3° (see Figure 2c), which is significantly different from the pure one (see Figure 2b). Besides, the surfaces of modified film are low adhesive. The H_2O droplet could not stick to the surface of the modified film and the sliding angle was <5°, which meant that the droplet was quite easy to roll off the surface. The low adhesive superhydrophobicity of the modified film is the result of the cooperation of the surface hierarchical structures and the low surface energy of silica.[47] We further tested the repellency of the modified film to the water and other corrosive liquids, which were common in the environment, because it was of vital importance for practical applications. Ut supra, the superhydrophobic film exhibited superior repellency to water (see Figure 2c and Supporting Information Figures S1 and S2). In addition, it also exhibited superior repellency toward corrosive liquids, for example, HCl, NaOH, etc. The static hydrophobic angles are almost the same regardless if the liquid is HCl, NaCl solution, or NaOH (pH ≤ 14) (see Figure 2d–f), demonstrating excellent repellency to the common corrosive liquids. We further applied this method to other kinds of nacre-mimetic films, such as MTM/PVP and graphene oxide (GO)/polymer, which also showed great repellency toward water in the environment (see Supporting Information Figure S3), proving this is a universal and facile method.

In addition to excellent repellency, the modification significantly improved the functionalities of the nacre-mimetic films. First of all, the gas barrier of the film was improved dramatically (see Table 1). As is well-known, many factors have

Table 1. Gas Barrier Property

gas permeability, $cm^3mm/m^2/day/atm$	pure	modified
He	1624.115	1.337
N_2	666.833	0.860
O_2	666.050	0.554
CO_2	535.629	0.159

an effect on the gas barrier properties of the films.[48−52] Thus, to minimize all the other factors that would affect the gas barrier properties and show the specific effect of coating, we compared the permeability of nacre-mimetic films before and after coating, which were both made of the same MTM/PVA by the same method. The result clearly showed that the oxygen and nitrogen permeability of the modified nacre-mimetic film (0.554 ± 0.020 and 0.860 ± 0.023 cm^3 mm m^{-2} day^{-1} atm^{-1}, respectively) were lowered by nearly 3 orders of magnitude when compared with pure MTM/PVA film (666.050 ± 242.050 and 666.833 ± 267.674 cm^3 mm m^{-2} day^{-1} atm^{-1}, respectively). The significant change is the result of a synergetic effect of triple (coating on both sides of the nacre-mimetic film) tortuous diffusive path and excellent superhydrophobic effect, which together improve the gas barrier of the film exponentially, a 1000 times improvement over the pristine films.[53−55] What's more, the oxygen permeability for the modified nacre-mimetic film was as low as 0.554 cm^3 mm m^{-2} day^{-1} atm^{-1}, which is among the best values for composites reported.[25,56] More importantly, the superhydrophobicity of the film makes the gas barrier property less related to the moisture when considering that it is often an important factor on the performance of other films. For instance, the oxygen permeability of pure PVA increases by a factor of over 5000 when exposed to water.[56] Thus, this modification method, which could improve the gas barrier property of the film and keep the transparency and flexibility of the film, would be of great value for films used in optoelectronic devices.

As is reported, nacre-mimetic films have great heat-shield and fire retardancy capabilities.[25,26,38] Thus, heat-shield and fire retardancy capabilities of nacre-mimetic films after modification were investigated to show the effect of coating. The resultant thermal conductivity of the modified film is very stable and as low as 42.58 ± 0.11 mW/(m K) at room temperature and 1 atm pressure, which is only 42.16% of the pure one (101.06 ± 1.78 mW/(m K)). From the date, it is easy to tell that the thermal conductivity of the modified one is very stable and decreased significantly (nearly as low as that of air) compared to the pure one and almost among the range of the best thermal insulation products of similar materials.[57,58] The excellent heat-shield property also could be evidenced when the modified film was exposed to a flame (see Figure 3 and Supporting Information videos S1 and S2). The flame caused a bright

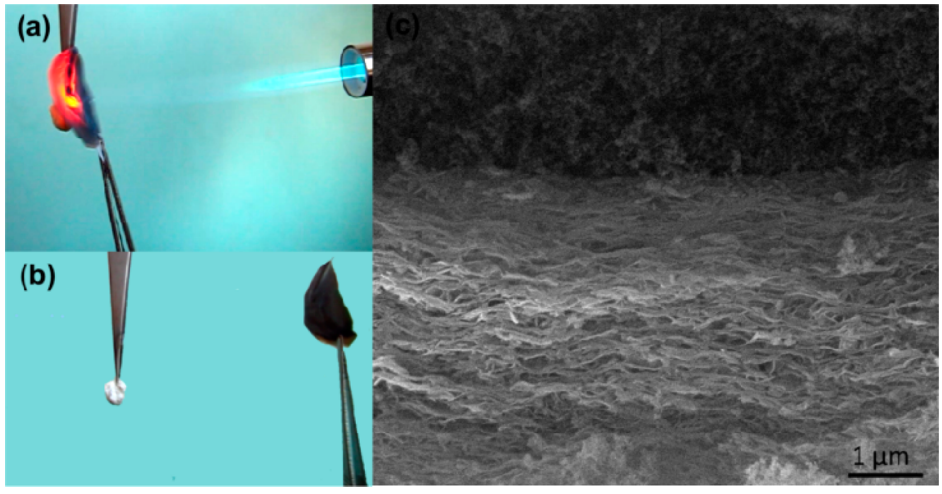

Figure 3. Flame and heat-shielding properties of modified MTM/PVA nacre-mimetic films. (a) Photograph of a film being exposed to a gas burner. (b) Nacre-mimetic paper used as a fire and heat shield to protect cotton. (For videos, see the Supporting Information videos S1 and S2.) (c) SEM image of the nacre paper after flame treatment (the layered structure of the film was almost preserved).

red glowing spot on the front of the films while there was much less brightness on the back, demonstrating great heat insulation. Detailed discussions about the flame-shield capability of the modified films can be seen in Supporting Information. To further illustrate the flame and heat-shield capabilities of the modified film, the film was placed between flammable cotton and high-temperature gas flames. The modified film successfully acted as an efficient thermal and flame shield to prevent the burning of the cotton. More interestingly, unlike the porous framework as reported before,[26,35] the layered structure of the film was almost preserved, which might show better thermal and flame-shield capabilities of the silica protective layer than those of the MTM/polymer system. The modification is very attractive for applications such as fascinating fire-protective films and coatings, because the thermal and flame-shield capabilities could be improved easily by simply adding more volume of as-prepared nanoparticle dispersion to form a thicker protective layer.

CONCLUSION

We have demonstrated a simple superhydrophobic modification method to enhance the repellency of the waterborne nacre-mimetic films to deposited liquids, to further advance the materials into practical applications. The modified films exhibited superior resistance toward water, with a contact angle of 151.5 ± 0.3°, and even toward corrosive liquids (HCl, NaOH, and aqueous salt solutions). This method also enhanced the gas barrier property of modified nacre-mimetic films by nearly 3 orders of magnitude. Besides, the thermal conductivity of the modified films was lowered to 42.58 ± 0.11 mW/(m K) from 101.06 ± 1.78 mW/(m K) and showed promising thermal and flame-shield capabilities. This easy, low-cost modification is also applicable to other kinds of nacre-mimetic materials, for example, multifunctional integrated graphene oxide (GO)/waterborne polymer and MTM/waterborne polymer composites, proving to be a universal, facile, and versatile avenue to produce lightweight materials with excellent repellency toward water and corrosive liquids in the environment and other superior properties. It is anticipated to be applied in a wide area of practical fields, such as in construction, transportation, and biomedical implant technology.

ASSOCIATED CONTENT

Supporting Information

Repellency of pure and modified films to water, comparison of the mechanical properties change during exposure to water, and repellency of modified MTM/PVP film and modified GO/polymer to water. Detailed discussions about flame-shield capability of the modified film. This material is available free of charge via the Internet at http://pubs.acs.org.

AUTHOR INFORMATION

Corresponding Author

*E-mail: guolin@buaa.edu.cn.

Notes

The authors declare no competing financial interest.

ACKNOWLEDGMENTS

The project is supported by the National Key Basic Research Program of China (2010CB934700).

REFERENCES

(1) Mayer, G. Rigid Biological Systems as Models for Synthetic Composites. *Science* **2005**, *310*, 1144−1147.
(2) Popat, K. C.; Porter, J. R.; Ruckh, T. T. Bone Tissue Engineering: A Review in Bone Biomimetics and Drug Delivery Strategies. *Biotechnol. Prog.* **2009**, *25*, 1539−1560.
(3) Ji, B. H.; Gao, H. J. Mechanical Principles of Biological Nanocomposites. *Annu. Rev. Mater. Res.* **2010**, *40*, 77−100.
(4) Studart, A. R. Towards High-Performance Bioinspired Composites. *Adv. Mater.* **2012**, *24*, 5024−5044.
(5) Wegst, U. G. K.; Ashby, M. F. The Mechanical Efficiency of Natural Materials. *Philos. Magn.* **2004**, *84*, 2167−2186.
(6) Sarikaya, M. An Introduction to Biomimetics: A Structural Viewpoint. *Microsc. Res. Technol.* **1994**, *27*, 360−375.
(7) Liu, K. S.; Jiang, L. Bio-Inspired Design of Multiscale Structures for Function Integration. *Nano Today* **2011**, *6*, 155−175.
(8) Yao, H. B.; Fang, H. Y.; Wang, X. H.; Yu, S. H. Hierarchical Assembly of Micro-/Nano-Building Blocks: Bio-Inspired Rigid Structural Functional Materials. *Chem. Soc. Rev.* **2011**, *40*, 3764−3785.
(9) Li, X. D.; Chang, W. C.; Chao, Y. J.; Wang, R. Z.; Chang, M. Nanoscale Structural and Mechanical Characterization of a Natural Nanocomposite Material: The Shell of Red Abalone. *Nano Lett.* **2004**, *4*, 613−617.
(10) Kamat, S.; Su, X.; Ballarini, R.; Heuer, A. H. Structural Basis for the Fracture Toughness of the Shell of the Conch Strombus Gigas. *Nature* **2000**, *405*, 1036−1040.
(11) Kakisawa, H.; Sumitomo, T. The Toughening Mechanism of Nacre and Structural Materials Inspired by Nacre. *Sci. Technol. Adv. Mater.* **2011**, *12*, 064710.
(12) Wang, J.; Cheng, Q.; Tang, Z. Layered Nanocomposites Inspired by the Structure and Mechanical Properties of Nacre. *Chem. Soc. Rev.* **2012**, *41*, 1111−1129.
(13) Corni, I.; Harvey, T. J.; Wharton, J. A.; Stokes, K. R.; Walsh, F. C.; Wood, R. J. K. A Review of Experimental Techniques to Produce a Nacre-Like Structure. *Bioinspiration Biomimetics* **2012**, *7*, 031001.
(14) Finnemore, A.; Cunha, P.; Shean, T.; Vignolini, S.; Guldin, S.; Oyen, M.; Steiner, U. Biomimetic Layer-by-Layer Assembly of Artificial Nacre. *Nat. Commun.* **2012**, *3*, 966.
(15) Li, Y.-Q.; Yu, T.; Yang, T.-Y.; Zheng, L.-X.; Liao, K. Bio-Inspired Nacre-Like Composite Films Based on Graphene with Superior Mechanical, Electrical, and Biocompatible Properties. *Adv. Mater.* **2012**, *24*, 3426−3431.
(16) Wang, J. F.; Lin, L.; Cheng, Q. F.; Jiang, L. A Strong Bio-Inspired Layered PNIPAM-Clay Nanocomposite Hydrogel. *Angew. Chem., Int. Ed.* **2012**, *51*, 4676−4680.
(17) Bonderer, L. J.; Studart, A. R.; Gauckler, L. J. Bioinspired Design and Assembly of Platelet Reinforced Polymer Films. *Science* **2008**, *319*, 1069−1073.
(18) Bonderer, L. J.; Studart, A. R.; Woltersdorf, J.; Pippel, E.; Gauckler, L. J. Strong and Ductile Platelet-Reinforced Polymer Films Inspired by Nature: Microstructure and Mechanical Properties. *J. Mater. Res.* **2009**, *24*, 2741−2754.
(19) Erb, R. M.; Libanori, R.; Rothfuchs, N.; Studart, A. R. Composites Reinforced in Three Dimensions by Using Low Magnetic Fields. *Science* **2012**, *335*, 199−204.
(20) Munch, E.; Launey, M. E.; Alsem, D. H.; Saiz, E.; Tomsia, A. P.; Ritchie, R. O. Tough, Bio-Inspired Hybrid Materials. *Science* **2008**, *322*, 1516−1520.
(21) Tang, Z. Y.; Kotov, N. A.; Magonov, S.; Ozturk, B. Nanostructured Artificial Nacre. *Nat. Mater.* **2003**, *2*, 413−418.
(22) Podsiadlo, P.; Kaushik, A. K.; Arruda, E. M.; Waas, A. M.; Shim, B. S.; Xu, J. D.; Nandivada, H.; Pumplin, B. G.; Lahann, J.; Ramamoorthy, A.; Kotov, N. A. Ultrastrong and Stiff Layered Polymer Nanocomposites. *Science* **2007**, *318*, 80−83.
(23) Podsiadlo, P.; Liu, Z. Q.; Paterson, D.; Messersmith, P. B.; Kotov, N. A. Fusion of Seashell Nacre and Marine Bioadhesive Analogs: High-Strength Nanocomposite by Layer-by-Layer Assembly of Clay and L-3,4-Dihydroxyphenylalanine Polymer. *Adv. Mater.* **2007**, *19*, 949−955.

(24) Podsiadlo, P.; Tang, Z. Y.; Shim, B. S.; Kotov, N. A. Counterintuitive Effect of Molecular Strength and Role of Molecular Rigidity on Mechanical Properties of Layer-by-Layer Assembled Nanocomposites. *Nano Lett.* **2007**, *7*, 1224−1231.
(25) Walther, A.; Bjurhager, I.; Malho, J. M.; Pere, J.; Ruokolainen, J.; Berglund, L. A.; Ikkala, O. Large-Area, Lightweight and Thick Biomimetic Composites with Superior Material Properties Via Fast, Economic, and Green Pathways. *Nano Lett.* **2010**, *10*, 2742−2748.
(26) Walther, A.; Bjurhager, I.; Malho, J. M.; Ruokolainen, J.; Berglund, L.; Ikkala, O. Supramolecular Control of Stiffness and Strength in Lightweight High-Performance Nacre-Mimetic Paper with Fire-Shielding Properties. *Angew. Chem., Int. Ed.* **2010**, *49*, 6448−6453.
(27) Burghard, Z.; Zini, L.; Srot, V.; Bellina, P.; van Aken, P. A.; Bill, J. Toughening through Nature-Adapted Nanoscale Design. *Nano Lett.* **2009**, *9*, 4103−4108.
(28) Shu, Y.; Yin, P.; Liang, B.; Wang, S.; Gao, L.; Wang, H.; Guo, L. Layer by Layer Assembly of Heparin/Layered Double Hydroxide Completely Renewable Ultrathin Films with Enhanced Strength and Blood Compatibility. *J. Mater. Chem.* **2012**, *22*, 21667−21672.
(29) Shu, Y. Q.; Yin, P. G.; Wang, J. F.; Liang, B. L.; Wang, H.; Guo, L. Bioinspired Nacre-Like Heparin/Layered Double Hydroxide Film with Superior Mechanical, Fire-Shielding, and UV-Blocking Properties. *Ind. Eng. Chem. Res.* **2014**, *53*, 3820−3826.
(30) Shu, Y.; Yin, P.; Liang, B.; Wang, H.; Guo, L. Bioinspired Design and Assembly of Layered Double Hydroxide/Poly(Vinyl Alcohol) Film with High Mechanical Performance. *ACS Appl. Mater. Interfaces* **2014**, *6*, 15154−15161.
(31) Laaksonen, P.; Walther, A.; Malho, J.-M.; Kainlauri, M.; Ikkala, O.; Linder, M. B. Genetic Engineering of Biomimetic Nanocomposites: Diblock Proteins, Graphene, and Nanofibrillated Cellulose. *Angew. Chem., Int. Ed.* **2011**, *50*, 8688−8691.
(32) An, Z.; Compton, O. C.; Putz, K. W.; Brinson, L. C.; Nguyen, S. T. Bio-Lnspired Borate Cross-Linking in Ultra-Stiff Graphene Oxide Thin Films. *Adv. Mater.* **2011**, *23*, 3842−3846.
(33) Putz, K. W.; Compton, O. C.; Palmeri, M. J.; Nguyen, S. T.; Brinson, L. C. High-Nanofiller-Content Graphene Oxide−Polymer Nanocomposites Via Vacuum-Assisted Self-Assembly. *Adv. Funct. Mater.* **2010**, *20*, 3322−3329.
(34) Zhang, L.; Wang, Z. P.; Xu, C.; Li, Y.; Gao, J. P.; Wang, W.; Liu, Y. High Strength Graphene Oxide/Polyvinyl Alcohol Composite Hydrogels. *J. Mater. Chem.* **2011**, *21*, 10399−10406.
(35) Cheng, Q.; Li, M.; Jiang, L.; Tang, Z. Bioinspired Layered Composites Based on Flattened Double-Walled Carbon Nanotubes. *Adv. Mater.* **2012**, *24*, 1838−1843.
(36) Shim, B. S.; Zhu, J.; Jan, E.; Critchley, K.; Ho, S. S.; Podsiadlo, P.; Sun, K.; Kotov, N. A. Multiparameter Structural Optimization of Single-Walled Carbon Nanotube Composites: Toward Record Strength, Stiffness, and Toughness. *ACS Nano* **2009**, *3*, 1711−1722.
(37) Wang, J.; Cheng, Q.; Lin, L.; Chen, L.; Jiang, L. Understanding the Relationship of Performance with Nanofiller Content in the Biomimetic Layered Nanocomposites. *Nanoscale* **2013**, *5*, 6356−6362.
(38) Yao, H. B.; Tan, Z. H.; Fang, H. Y.; Yu, S. H. Artificial Nacre-Like Bionanocomposite Films from the Self-Assembly of Chitosan-Montmorillonite Hybrid Building Blocks. *Angew. Chem., Int. Ed.* **2010**, *49*, 10127−10131.
(39) Wang, C. A.; Long, B.; Lin, W.; Huang, Y.; Sun, J. L. Polyacrylamide−Clay Nacre-Like Nanocomposites Prepared by Electrophoretic Deposition. *Compos. Sci. Technol.* **2007**, *67*, 2770−2774.
(40) Das, P.; Schipmann, S.; Malho, J.-M.; Zhu, B.; Klemradt, U.; Walther, A. Facile Access to Large-Scale, Self-Assembled, Nacre-Inspired, High-Performance Materials with Tunable Nanoscale Periodicities. *ACS Appl. Mater. Interfaces* **2013**, *5*, 3738−3747.
(41) Verho, T.; Karesoja, M.; Das, P.; Martikainen, L.; Lund, R.; Alegría, A.; Walther, A.; Ikkala, O. Hydration and Dynamic State of Nanoconfined Polymer Layers Govern Toughness in Nacre-Mimetic Nanocomposites. *Adv. Mater.* **2013**, *25*, 5055−5059.
(42) Xu, L.-P.; Peng, J.; Liu, Y.; Wen, Y.; Zhang, X.; Jiang, L.; Wang, S. Nacre-Inspired Design of Mechanical Stable Coating with Underwater Superoleophobicity. *ACS Nano* **2013**, *7*, 5077−5083.
(43) Xu, L.-P.; Zhao, J.; Su, B.; Liu, X.; Peng, J.; Liu, Y.; Liu, H.; Yang, G.; Jiang, L.; Wen, Y.; Zhang, X.; Wang, S. An Ion-Induced Low-Oil-Adhesion Organic/Inorganic Hybrid Film for Stable Superoleophobicity in Seawater. *Adv. Mater.* **2013**, *25*, 606−611.
(44) Kochumalayil, J. J.; Morimune, S.; Nishino, T.; Ikkala, O.; Walther, A.; Berglund, L. A. Nacre-Mimetic Clay/Xyloglucan Bionanocomposites: A Chemical Modification Route for Hygromechanical Performance at High Humidity. *Biomacromolecules* **2013**, *14*, 3842−3849.
(45) Das, P.; Walther, A. Ionic Supramolecular Bonds Preserve Mechanical Properties and Enable Synergetic Performance at High Humidity in Water-Borne, Self-Assembled Nacre-Mimetics. *Nanoscale* **2013**, *5*, 9348−9356.
(46) Xue, B.; Li, X.; Gao, L.; Gao, M.; Wang, Y.; Jiang, L. CO_2-Selective Free-Standing Membrane by Self-Assembly of a UV-Crosslinkable Diblock Copolymer. *J. Mater. Chem.* **2012**, *22*, 10918−10923.
(47) Su, B.; Wang, S.; Song, Y.; Jiang, L. A Miniature Droplet Reactor Built on Nanoparticle-Derived Superhydrophobic Pedestals. *Nano Res.* **2010**, *4*, 266−273.
(48) Holder, K. M.; Priolo, M. A.; Secrist, K. E.; Greenlee, S. M.; Nolte, A. J.; Grunlan, J. C. Humidity-Responsive Gas Barrier of Hydrogen-Bonded Polymer−Clay Multilayer Thin Films. *J. Phys. Chem. C* **2012**, *116*, 19851−19856.
(49) Tzeng, P.; Maupin, C. R.; Grunlan, J. C. Influence of Polymer Interdiffusion and Clay Concentration on Gas Barrier of Polyelectrolyte/Clay Nanobrick Wall Quadlayer Assemblies. *J. Membr. Sci.* **2014**, *452*, 46−53.
(50) Priolo, M. A.; Holder, K. M.; Greenlee, S. M.; Grunlan, J. C. Transparency, Gas Barrier, and Moisture Resistance of Large-Aspect-Ratio Vermiculite Nanobrick Wall Thin Films. *ACS Appl. Mater. Interfaces* **2012**, *4*, 5529−5533.
(51) Priolo, M. A.; Holder, K. M.; Greenlee, S. M.; Stevens, B. E.; Grunlan, J. C. Precisely Tuning the Clay Spacing in Nanobrick Wall Gas Barrier Thin Films. *Chem. Mater.* **2013**, *25*, 1649−1655.
(52) Xiang, F. M.; Tzeng, P.; Sawyer, J. S.; Regev, O.; Grunlan, J. C. Improving the Gas Barrier Property of Clay−Polymer Multilayer Thin Films Using Shorter Deposition Times. *ACS Appl. Mater. Interfaces* **2014**, *6*, 6040−6048.
(53) Sehaqui, H.; Kochumalayil, J.; Liu, A. D.; Zimmermann, T.; Berglund, L. A. Multifunctional Nanoclay Hybrids of High Toughness, Thermal, and Barrier Performances. *ACS Appl. Mater. Interfaces* **2013**, *5*, 7613−7620.
(54) Yang, Y. H.; Bolling, L.; Priolo, M. A.; Grunlan, J. C. Super Gas Barrier and Selectivity of Graphene Oxide−Polymer Multilayer Thin Films. *Adv. Mater.* **2013**, *25*, 503−508.
(55) Sangermano, M.; Malucelli, G.; Amerio, E.; Priola, A.; Billi, E.; Rizza, G. Photopolymerization of Epoxy Coatings Containing Silica Nanoparticles. *Prog. Org. Coat.* **2005**, *54*, 134−138.
(56) Lagaron, J. M.; Catala, R.; Gavara, R. Structural Characteristics Defining High Barrier Properties in Polymeric Materials. *Mater. Sci. Technol.* **2004**, *20*, 1−7.
(57) Tomasi, R.; Sireude, D.; Marchand, R.; Scudeller, Y.; Guillemet, P. Preparation of a Thermal Insulating Material Using Electrophoretic Deposition of Silica Particles. *Mater. Sci. Eng., B* **2007**, *137*, 225−231.
(58) Chen, Q.; Wang, S.; Li, Z. Fabrication and Characterization of Aluminum Silicate Fiber−Reinforced Hollow Mesoporous Silica Microspheres Composites. *Microporous Mesoporous Mater.* **2012**, *152*, 104−109.